



저작자표시-비영리-변경금지 2.0 대한민국

이용자는 아래의 조건을 따르는 경우에 한하여 자유롭게

- 이 저작물을 복제, 배포, 전송, 전시, 공연 및 방송할 수 있습니다.

다음과 같은 조건을 따라야 합니다:



저작자표시. 귀하는 원저작자를 표시하여야 합니다.



비영리. 귀하는 이 저작물을 영리 목적으로 이용할 수 없습니다.



변경금지. 귀하는 이 저작물을 개작, 변형 또는 가공할 수 없습니다.

- 귀하는, 이 저작물의 재이용이나 배포의 경우, 이 저작물에 적용된 이용허락조건을 명확하게 나타내어야 합니다.
- 저작권자로부터 별도의 허가를 받으면 이러한 조건들은 적용되지 않습니다.

저작권법에 따른 이용자의 권리는 위의 내용에 의하여 영향을 받지 않습니다.

이것은 [이용허락규약\(Legal Code\)](#)을 이해하기 쉽게 요약한 것입니다.

[Disclaimer](#)

Doctor of Philosophy

Magnetically Guided Targeted Drug Delivery  
System of Erythropoietin Using Magnetic  
Nanoparticles: Proof of Concept

The Graduate School  
of the University of Ulsan  
Department of Physical  
Medicine and Rehabilitation  
Kim, Chung Reen

Magnetically Guided Targeted Drug Delivery  
System of Erythropoietin Using Magnetic  
Nanoparticles: Proof of Concept

Supervisor : Hwang, Chang Ho

A Dissertation

Submitted to  
the Graduate School of the University of Ulsan  
In partial Fulfillment of the Requirements  
for the Degree of

Doctor of Philosophy in Medicine

by

Kim, Chung Reen

Department of Physical  
Medicine and Rehabilitation  
Ulsan, Korea  
February 2020

Magnetically Guided Targeted Drug Delivery  
System of Erythropoietin Using Magnetic  
Nanoparticles: Proof of Concept

This certifies that the dissertation  
of Kim, Chung Reen is approved.

---

Committee Chair Dr. Yang, Dong Seok

---

Committee Member Dr. Hwang, Chang Ho

---

Committee Member Dr. Jung, Kwang Hwan

---

Committee Member Dr. Kang, Byeong Seong

---

Committee Member Dr. Lee, Jong Hwa

Department of Physical  
Medicine and Rehabilitation  
Ulsan, Korea  
February 2020

## ABSTRACT

**Purpose:** The objective of this proof-of-concept study was to demonstrate the targeted delivery of erythropoietin (EPO) using magnetically guided magnetic nanoparticles (MNPs).

**Materials and Methods:** MNPs consisting of a ferric-ferrous mixture ( $\text{FeCl}_3 \cdot 6\text{H}_2\text{O}$  and  $\text{FeCl}_2 \cdot 4\text{H}_2\text{O}$ ) were prepared using a co-precipitation method. The drug delivery system (DDS) was manufactured via the spray-drying technique using a nanospray-dryer. The DDS comprised 7.5 mg sodium alginate, 150 mg MNPs, and 1000 IU EPO.

**Results:** Scanning electron microscopy revealed DDS particles no more than 500 nm in size. Tiny particles on the rough surfaces of the DDS particles were composed of MNPs and/or EPO, unlike the smooth surfaces of the only alginate particles. Fourier-transform infrared spectroscopy revealed DDS peaks characteristic of MNPs as well as of alginate. Standard soft lithography was applied to DDS particles prepared with fluorescent beads using a microchannel fabricated to have one inlet and two outlets in a Y-shape. The fluorescent DDS particles reached only one outlet reservoir in the presence of a neodymium magnet. The neurotoxicity was evaluated by treating SH-SY5Y cells in 48-well plates ( $1 \times 10^5$  cells/well) with 2  $\mu\text{L}$  of a solution containing sodium alginate (0.075 mg/mL), MNPs (1.5 mg/mL), or sodium alginate + MNPs. A cell viability assay kit was used to identify a 93% cell viability after MNP treatment and a 94% viability after sodium alginate + MNP treatment, compared with the control ( $p < 0.01$ ).

**Conclusions:** The DDS-EPO construct developed here can be guided using magnetic control without displaying significant neurotoxicity.

**Keywords:** erythropoietin; magnetics; nanoparticles; neurotoxicity; regeneration

## CONTENTS

ABSTRACT .....	i
LISTS OF FIGURES .....	iii
INTRODUCTIONS .....	1
MATERIALS AND METHODS .....	3
1. Synthesizing magnetic nanoparticles .....	3
2. Drug delivery system fabrication using a nanospray dryer .....	5
3. Characterization of the drug delivery system particles .....	7
3.1. Scanning electron microscopy .....	7
3.2. Fourier-transform infrared spectroscopy .....	7
4. Magnetic guidance of the drug delivery system .....	7
5. The neurotoxicity of the magnetic nanoparticles .....	7
6. Statistical analysis .....	8
RESULTS .....	9
1. Scanning electron microscopy .....	9
2. Fourier-transform infrared spectroscopy .....	9
3. Magnetic guidance of the drug delivery system .....	12
4. The neurotoxicity of magnetic nanoparticles .....	12
DISCUSSION .....	15
CONCLUSIONS .....	20
REFERENCES .....	21
APPENDIX .....	26
KOREAN ABSTRACTS .....	27

## LISTS OF FIGURES

Fig. 1. Schematic diagram of the magnetically guided targeted delivery of erythropoietin	4
Fig. 2. Nanospray dryer	6
Fig. 3. Scanning electron microscopy	10
Fig. 4. Fourier-transform infrared spectroscopy	11
Fig. 5. Magnetic guidance of the drug delivery system	13
Fig. 6. The Neurotoxicity of the magnetic nanoparticles	14

## INTRODUCTION

Central nervous system (CNS) injuries, including brain and spinal cord injury, cause serious sequelae in most patients and increase the medical costs associated with individuals and nations. Among the various therapeutic strategies against CNS injuries currently under development,<sup>1</sup> erythropoietin (EPO) has been tested in *in vitro/in vivo* experiments in brain and spinal cord injury models.<sup>2-6</sup> Neuro-protection or -regeneration in the presence of EPO has been evaluated since early 2000s.<sup>1, 7</sup> The widespread use of EPO in hematologic diseases suggests that it may be more readily applicable to CNS injury patients than other experimental drugs.<sup>8</sup> Unfortunately, the therapeutic time window within which EPO may be effective against CNS injury is very limited (no more than 6 hours after injury),<sup>9</sup> and few clinical trials have obtained high-quality evidence supporting the efficacy of its use. In the study of acute stroke patients, no significant improvement in the Barthel index was observed in the EPO group compared to the control group, but mortality was higher in the EPO group.<sup>10</sup> Although significant improvements in functional outcomes were observed in patients with spinal cord injury, it was studied in the case of administration within 6 hours after injury.<sup>11</sup> Even when EPO was administered in moderate to severe traumatic brain injury, erythropoietin did not decrease the number of patients with severe neurological dysfunction, but rather increased the incidence of deep venous thrombosis of the lower limbs.<sup>12</sup> Thus, clinical studies to date have not shown positive results, unlike animal experiments, but rather caused serious side effects. Although the positive effect could be expected when administered to spinal cord injury patients, short therapeutic window time needs to be resolved. Additionally, hematopoietic and non-hematopoietic EPO receptors display significant heterogeneity and phylogenetic differences in human beings.<sup>13</sup> Efficient action requires EPO to escape binding at *non-in situ* EPO receptors. To demonstrate clinical feasibility in urgent CNS injury situations, it is essential to ensure very fast targeted delivery to an injured area.

Drug delivery systems (DDS) have been widely investigated in recent years. In a stroke model study of DDS with nanoerythropoietin, Chen et al. reported that treatment with erythropoietin nano-drug was 10 times more effective than erythropoietin.<sup>14</sup> It was thought



that the nanoformulation might stabilize the EPO and promote blood brain barrier crossing. Also, DDS using nanoparticles has the advantage of being able to mix and administer the desired substances as well as therapeutic drugs. In particular, if the magnetic substance is mixed together, the magnet can be used to collect the drug in the desired position, thereby maximizing the action of the drug. In the previous study, magnetic-guided navigation is advantageous in its ability to guide magnetic nanoparticles (MNPs) and successfully penetrate the blood-brain barriers (BBBs) in *in vivo* rat models.<sup>15</sup> The results showed that magnetic-guided navigation can increase additional effects of drug, and therefore, its usefulness is considered to be promising.

Colloidal MNP solutions are stable in the presence of organic materials, such as fatty acids or polysaccharides, during delivery to targeted areas. Magnetic DDS using MNPs may be one of the most promising DDS methods identified to date.<sup>16</sup> However, when DDS is prepared by mixing only MNP and erythropoietin, it is easily aggregated by external stimulation such as pH and temperature, and thus a substance capable of stabilizing the conjugate is required. Among those substances, sodium alginate is a widely used, natural, non-toxic, biodegradable polymer ( $\alpha$ -L-galuronic acid units and (1,4)-linked  $\beta$ -D-mannuronic acid units).<sup>17</sup>

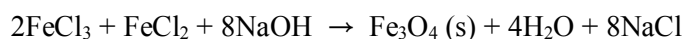
This work sought to demonstrate a new therapeutic strategy against CNS injury utilizing the rapid delivery of a combination of EPO and MNPs to injured sites within a therapeutic time window and the localization of these constructs exclusively within the injured area with aid of external magnetic field guidance, to avoid competition with other EPO receptors outside of the injured sites. As proof-of-concept, the authors manufactured a DDS comprising biodegradable alginate-coated EPO-nanoparticle polymers using a nanospray drying technique. The particles were then encapsulated and characterized in terms of their size, degree of encapsulation, amenability to magnetic guidance, and neuronal cell toxicity.

## MATERIALS AND METHODS

First, MNPs to be used for DDS were synthesized, and then DDS was prepared using the spray-drying technique with recombinant human erythropoietin (rhEPO), MNPs and sodium alginate. Finally, the size, shape, and configuration of the fabricated DDS were verified. And it was confirmed whether the DDS with MNPs was well induced by the magnet. We also confirmed the neurotoxicity of MNPs and sodium alginate. Schematic diagram of the magnetically guided targeted delivery of erythropoietin was described in Figure 1.

### *1. Synthesizing magnetic nanoparticles*

MNPs were synthesized using a chemical co-precipitation method, the most widely used method for synthesizing MNPs.<sup>18</sup> Fe<sub>3</sub>O<sub>4</sub> MNPs were prepared via the chemical co-precipitation of Fe<sup>3+</sup> and Fe<sup>2+</sup> ions in a molar ratio of 2 : 1 under basic conditions. The MNP synthesis reaction could be expressed as:



Ferric chloride hexahydrate (FeCl<sub>3</sub>·6H<sub>2</sub>O) and ferrous chloride tetrahydrate (FeCl<sub>2</sub>·4H<sub>2</sub>O) were obtained from Sigma-Aldrich, S. Louis, USA. In 100 mL distilled (DI) water, 0.02 mol/L FeCl<sub>3</sub>·6H<sub>2</sub>O and 0.01 mol/L FeCl<sub>2</sub>·4H<sub>2</sub>O were dissolved to form a homogeneous solution in a 250 mL glass beaker. An NaOH (Kanto, Tokyo, Japan) solution was prepared (0.8 mol/L in DI water) over 30 minutes. The ferric-ferrous mixture was stirred at 500 rpm, and the NaOH solution was slowly added to this solution using a syringe pump at a flow rate of 1.0 mL/min under oxygen-free conditions at room temperature. The pH value was measured continuously, and NaOH delivery was stopped once the pH reached 10.5.<sup>19</sup> Following completion of the NaOH reaction, the mixture was stirred continuously for 3 hours. Subsequently, MNPs (black suspended particles) in the solution were magnetically filtered using a strong permanent magnet. The supernatant containing residual chemicals was

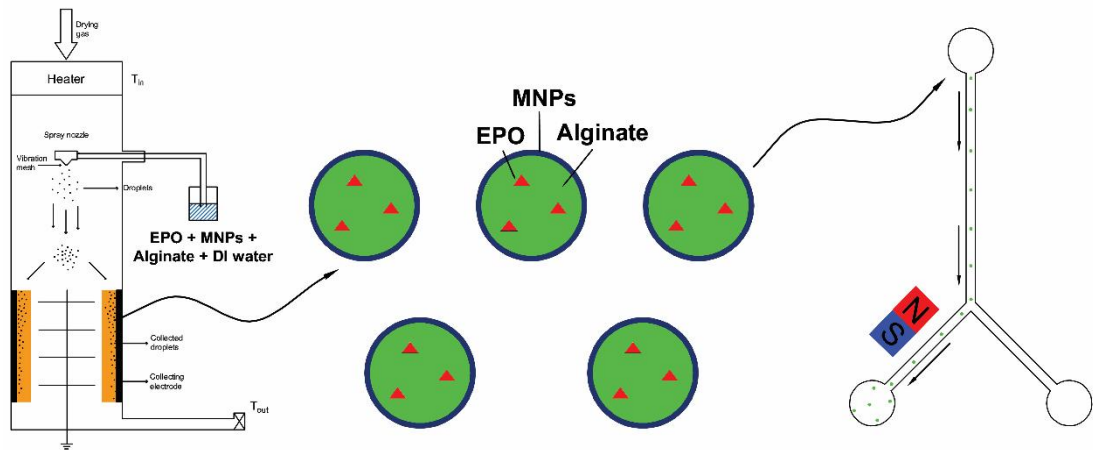


Fig. 1. Schematic diagram of the magnetically guided targeted delivery of erythropoietin.

removed. The filtered MNPs were washed several times with DI water to reach a neutral pH. The neutral MNPs were dried at 80°C overnight. Finally, the dried MNPs were annealed at 400°C for 2 hours.

## ***2. Drug delivery system fabrication using a nanospray dryer***

The alginate-encapsulated EPO-MNPs were manufactured via a spray-drying technique using a nanospray dryer B-90 (Fig. 2: Büchi Labortechnik AG, Flawil, Switzerland). The nanospray dryer included a pulsating casing in the spray nozzle to atomize the feed, and an electrostatic particle accumulator gathered the particles.<sup>20</sup> This study used a small spray nozzle (4 µm). The flow rate was set to 102–106 L/min, and the relative spray rate was fixed at 80% with an aspirator flow rate of 27.3 m<sup>3</sup>/min. The inlet temperature and outlet temperature were set to 120°C and 40°C, respectively with a pressure of 28 mbar.

The alginate solution (Chem-Supply, Gillman, Australia) was mixed with the MNPs and rhEPO (Epoetin alfa; Sigma-Aldrich, S. Louis, USA). First, 7.5 mg sodium alginate and 150 mg MNPs were added to a beaker containing 100 mL DI water, and the solution was sonicated for 1 hour. One milliliter 1000 IU rhEPO was added to the mixture of MNPs and sodium alginate, and the mixture was stirred for 30 minutes. The final solution was filtered prior to applying the spray-drying process to avoid nozzle blockage. The solution was sprayed over 1 hour. The dried particles were collected from the particle chamber using a powder scraper, which dispersed the DDS. The dried particles comprised 7.5 mg sodium alginate, 150 mg MNPs, and 1000 IU rhEPO. The particles were stored in a desiccator at a temperature of 25°C. The neuro-protective concentrations reported previously suggested that EPO should be diluted at 10 IU/mL.<sup>21-23</sup> A 10 IU/mL rhEPO solution was prepared by dissolving the collected DDS particles in 1 mL DI water and diluting the solution to 1/100. The concentrations of sodium alginate and the MNPs were also diluted to 0.075 mg/mL and 1.5 mg/mL.



Fig. 2. Nanospray dryer.

### ***3. Characterization of the drug delivery system particles***

#### ***3.1 Scanning electron microscopy***

The sizes, shapes, and surface aspects of the synthesized MNPs, that is, the spray-dried alginate and spray-dried DDS, were evaluated using scanning electron microscopy (SEM; SU8220, Hitachi, Tokyo, Japan). The particles were sputter-coated with platinum to enhance the surface conductivity prior to scanning and were analyzed at a voltage of 5.0 kV. The average size was calculated from a set of more than 100 particles imaged by SEM.

#### ***3.2 Fourier-transform infrared spectroscopy***

Fourier-transform infrared (FTIR) spectroscopy (Nicolet iS5, Thermo Fisher Scientific, Waltham, USA) was conducted to confirm the formation of the DDS by measuring the characteristic peaks. The sample pellets were prepared by blending with potassium bromide (KBr) and then compressing. The transmission spectra were obtained from 400 to 4000  $\text{cm}^{-1}$  with a resolution of 4  $\text{cm}^{-1}$ .

### ***4. Magnetic guidance of the drug delivery system***

Standard soft lithography was used to prepare a bifurcated microchannel and demonstrate magnetic guidance of the DDS. The lithography process was used to fabricate a simple polydimethylsiloxane (PDMS) bifurcated microchannel to mimic blood vessel microchannels. The bifurcated microchannel was designed to have one inlet channel and two outlet bifurcation channels in an inverted Y-shape. The width and height of the channel were 200  $\mu\text{m}$ , and the angle between the two channel branches was 90°. A neodymium magnet was placed near the right outlet channel to guide the DDS droplets.

Fluorescence microbeads were added to the DDS. Gelation was ensured by soaking the DDS in  $\text{CaCl}_2$  for 30 minutes prior to mixing with phosphate-buffered saline (PBS). The gelated DDS were mixed with PBS at a concentration of 10 mg/mL and injected into the inlet port of the bifurcated microchannel. Fluorescence microscopy was used to monitor the movement of the DDS during magnetic guidance tests.

### ***5. The neurotoxicity of the magnetic nanoparticles***

Prior to evaluating the neuroprotective effects of the DDS containing rhEPO, the neurotoxicity of the MNPs in the DDS was tested. The SH-SY5Y cell line, a human-derived neuronal cell line widely used in experimental neurological studies, was used for this purpose.<sup>24</sup> SH-SY5Y cells (Sigma-Aldrich, S. Louis, MO, USA) were plated into 48-well plates at  $1 \times 10^5$  cells/well. Cells were incubated for 24 hours in a CO<sub>2</sub> incubator.

During incubation, three different solutions containing DI water were prepared as followed: MNP solution (150 mg/mL), alginate solution (7.5 mg/mL) and MNP + alginate solution (150 mg/mL MNP and 7.5 mg/mL alginate). The DI water used to prepare the solutions was sterilized by filtering through a 0.2  $\mu$ m pore size membrane. All three solutions were sonicated for 1 hour at room temperature. Twenty-four hours after plating, the media of each well was replaced with 200  $\mu$ L Dulbecco's Modified Eagle's medium (DMEM). As previously mentioned, the target concentrations of MNP and sodium alginate in the well were 0.075 mg/mL and 1.5 mg/mL, respectively. The 200  $\mu$ L DMEM containing the incubated SH-SY5Y cells were treated with 2  $\mu$ L sodium alginate solution, 2  $\mu$ L MNP solution, or 2  $\mu$ L sodium MNP + alginate solution.

The treated cells were incubated for 22 hours in a CO<sub>2</sub> incubator, and 20  $\mu$ L EZ-cytox reagent (DoGenBio, Seoul, South Korea) was added to each well. The cells were then incubated for an additional 2 hours. The treated cell viability was determined using a microplate reader that measured the absorbance at 450 nm using the EZ-cytox cell viability assay kit (DoGen, Seoul, South Korea).

## ***6. Statistical Analysis***

In cell viability assay, optical density values were calculated using separate analyses using one-way analysis of variance (ANOVA). Significance was defined as  $<0.01$  compared with the control group.

## RESULTS

### *1. Scanning electron microscopy*

Figure 3 presents the morphologies of the synthesized MNPs, spray-dried alginate, and DDS prepared using the proposed methods. The size of synthesized MNPs, spray-dried alginate, and DDS is 0.03  $\mu\text{m}$  or less, 0.1-0.5  $\mu\text{m}$ , and 0.1-0.9  $\mu\text{m}$ , respectively. Spray-dried alginate particles were spherical in shape with smooth surfaces. SEM images indicated that the MNPs and EPO were well mixed with the alginate, and both or either component formed a rough surface on the DDS particles.

### *2. Fourier-transform infrared spectroscopy*

FTIR spectroscopy was used to confirm the formation of the DDS by measuring the characteristic peaks (Fig. 4). The FT-IR spectrum of the MNPs (Fig. 4A) revealed a vibrational Fe-O peak at 598–628  $\text{cm}^{-1}$ , confirming MNPs formation.<sup>25</sup> Another characteristic peak at 1632  $\text{cm}^{-1}$ , corresponding to O-H bending, demonstrated the presence of hydroxyl groups on the MNP surfaces. These results highlighted the presence of  $\text{Fe}(\text{OH})_2$  on the MNP surfaces, which formed during the passivation and stabilization of the MNPs. Figure 4B shows the FTIR spectra of the spray-dried alginate (i) and DDS (ii). Compared with the spray-dried alginate, the DDS included all peaks characteristic of the spray-dried alginate, as expected. The DDS, however, also included peaks characteristic of Fe-O at 589–630  $\text{cm}^{-1}$ , confirming the presence of MNPs on the DDS. A slight shift in the Fe-O peak was noted, from 598–628  $\text{cm}^{-1}$  to 580–630  $\text{cm}^{-1}$ , attributed to the MNP size reduction during DDS formation due to prolonged sonication. The characteristic peaks are listed in Supplement table 1.<sup>26, 27</sup>



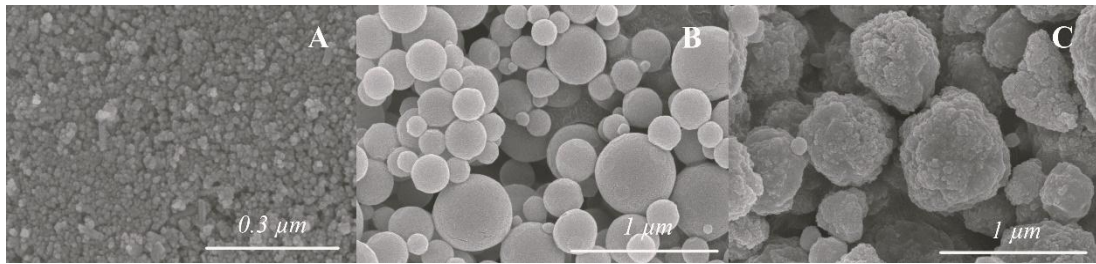


Fig. 3. Scanning electron microscopy. Scanning electron microscopy images showing (A) the synthesized magnetic nanoparticles, (B) the spray-dried alginate, and (C) the drug delivery system composed of magnetic nanoparticles, alginate, and erythropoietin. The magnetic nanoparticles and erythropoietin were well mixed with alginate, and both components formed a rough surface on the drug delivery system particles.

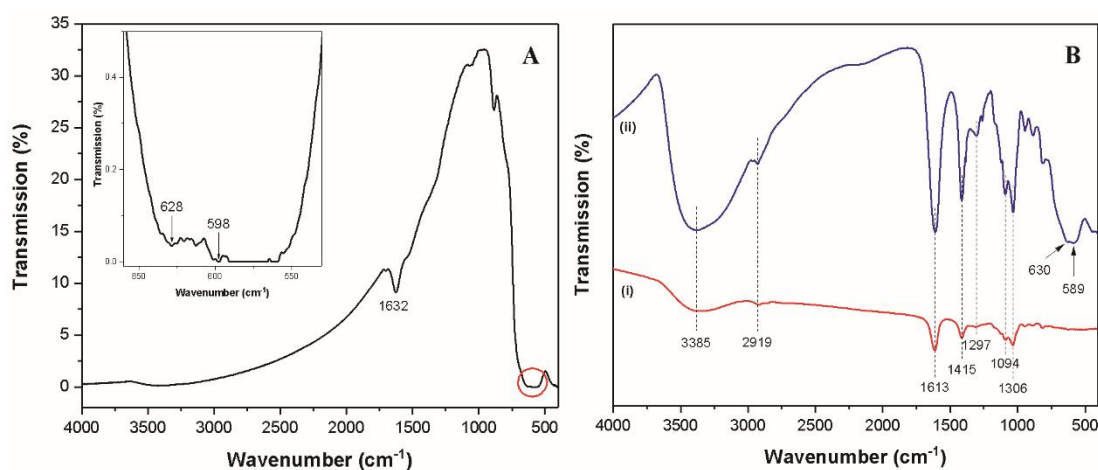


Fig. 4. Fourier-transform infrared spectroscopy. The Fourier-transform infrared spectra showed (A) the synthesized magnetic nanoparticles, (B) the spray-dried alginate (i), and the drug delivery system composed of magnetic nanoparticles, alginate, and erythropoietin (ii). The Fourier-transform infrared spectra of the spray-dried alginate and drug delivery system showed that the drug delivery system Fourier-transform infrared spectrum featured a peak characteristic of Fe-O at  $589\text{--}630\text{ cm}^{-1}$ , confirming the presence of magnetic nanoparticles and alginate on the drug delivery system.

### ***3. Magnetic guidance of the drug delivery system***

Figure 5 shows the results of the magnetic guidance experiments. On the right side of the bifurcated PDMS microchannels (Fig. 5A), the permanent magnet was positioned to impose a magnetic field. (The magnet is not shown in Fig. 5A.) The DDS particles prepared with fluorescent beads were injected using a syringe pump through the inlet of the PDMS microchannel (the upper branch of Fig. 5A). The injected velocity was 0.3 mL/min. The fluorescent DDS particles reached the right outlet reservoir of the PDMS microchannel (Fig. 5B). The left outlet reservoir harvested trace amount of DDS (Fig. 5C).

### ***4. The neurotoxicity of magnetic nanoparticles***

Figure 6 presents the SH-SY5Y neuronal cell viability test results for each of the three materials. The alginate-only solution did not cause cell death, as expected. Compared with the control, 1.5 mg/mL MNPs displayed a cell viability that was approximately 7% lower than that of the control. The mixture of alginate and MNPs yielded a slightly higher cell viability (about 1% higher than that of the control).

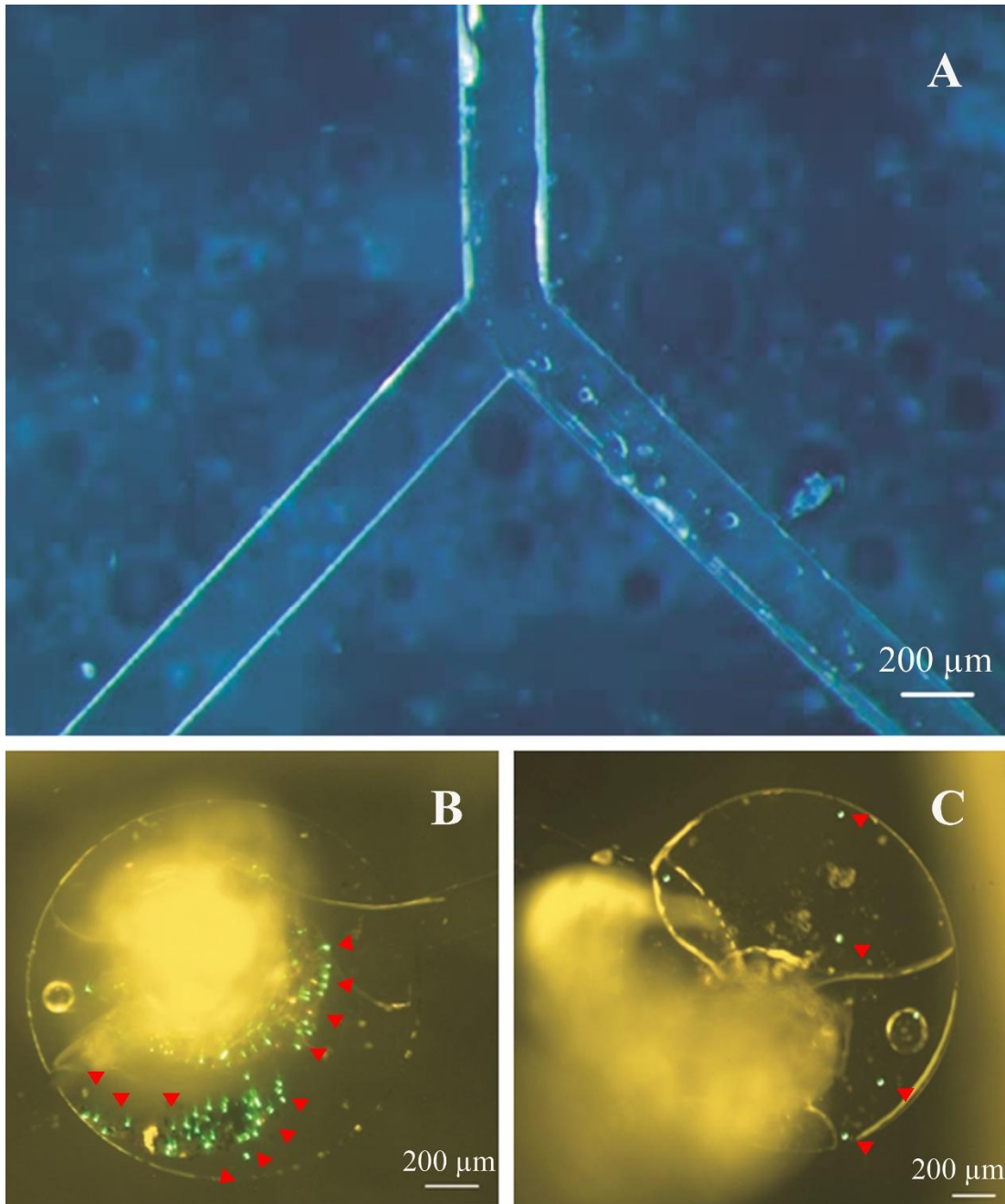


Fig. 5. Magnetic guidance of the drug delivery system. Drug delivery system guidance experiment results. (A) Bifurcated polydimethylsiloxane microchannel. The magnet was positioned in the right area of the microchannel but is not shown. (B) Magnetically guided fluorescent drug delivery system particles (red arrow head). (C) Trace amount of drug delivery systems was harvested in the absence of guidance.

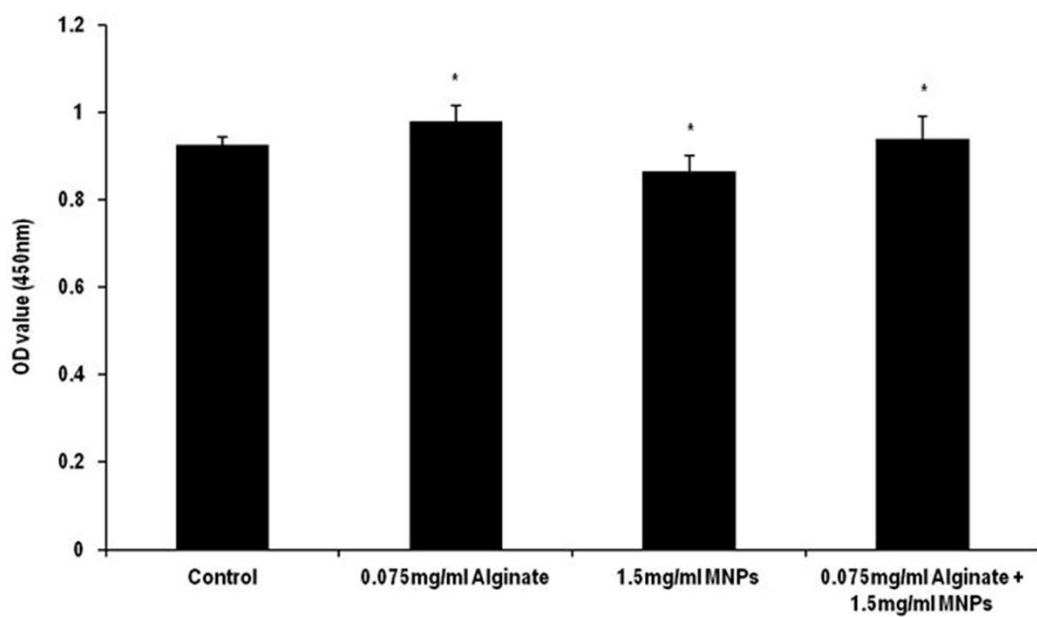


Fig. 6. Neurotoxicity of the magnetic nanoparticles, tested using the SH-SY5Y cells. The SH-SY5Y neuronal cell viabilities of the three materials were compared. No significant cytotoxicity was observed for the alginate, magnetic nanoparticles, and drug delivery systems. OD; optical density, \* $p < 0.01$  compared with the control.

## DISCUSSION

### *1. Significance of the method with respect to existing/alternative methods*

EPO is expected to compete for binding at a heterogeneous collection of phylogenetically distinct hematopoietic and non-hematopoietic EPO receptors.<sup>13,28</sup> Only a limited quantity of EPO is expected to reach an injured site following conventional administration. Therefore, it is necessary to reduce the chance that the administered EPO can bind to the hematopoietic receptor or the non-hematopoietic EPO receptor away from the injury site, and focus on the desired site. For this purpose, our concept of magnetic-guided navigation is expected to help improve the above problems in that the administered DDS can be collected around the magnetic control. Especially, the very short therapeutic time window for EPO (< 6 hours) must be considered in *in vivo* CNS injury situations.<sup>9,29,30</sup> Systemic circulation takes only a few minutes, such that the DDS is expected to provide EPO a hundred chances to reach an injured site and remain there in a high density under magnetic control. To the best of our knowledge, the directed targeted delivery of EPO using magnetic guidance represents a departure from the approaches of most recent trials, which focused on the slow sustained release of EPO from DDS particles.<sup>31</sup>

Few prior reports have described targeted EPO delivery, and the methods that do describe such approaches are, in fact, indirect, for example, inducing BBB crossing using focused ultrasound sonication with micro-bubbles or epi-cortical implantation and delivery following craniotomy.<sup>30,32</sup> By contrast, the DDS presented here is capable of targeting the delivery of EPO directly under magnetic guidance to increase the amount of EPO available for neuro-protective action and overcome the current drawbacks of EPO DDS, including *in vivo* competition by receptor binding after delivery.<sup>33, 34</sup> Furthermore, prior MNP-incorporated DDS trials examining the delivery of EPO did not evaluate targeted delivery; rather, they examined only the synergistic/additive effects of MNP with EPO.<sup>14, 31, 35</sup> Although nanoparticles alone can impart neuro-protective or neuro-regenerative effects by stimulating neuronal regrowth, improving neuronal survivability, or promoting neuronal differentiation,<sup>36</sup> the combination of nanoparticles and EPO has been shown to be 10 times as neuro-protective as rhEPO in ischemic rat models.<sup>14</sup> Unlike our study, previous study did not

attempt to induce drugs using magnets. However, we expected that drug induction using magnets will readily concentrate erythropoietin DDS in the desired area, thus it will be more effective than simply using nanoparticles in the treatment of CNS injury. Therefore, future studies will continue to study erythropoietin using magnetic DDS *in vitro* and *in vivo*. Especially, the combination of EPO and MNPs may be more promising than another magnetic mediator, magnetosomes.<sup>37</sup>

## ***2. Modifications and troubleshooting***

In considering the type of erythropoietin for this experiment, both murine EPO and rhEPO were considered. Although previous *in vivo* animal experiments used commonly both murine EPO and rhEPO, a nucleotide sequence analysis revealed that murine EPO showed only 80% homology with human EPO.<sup>38</sup> Therefore, rhEPO was selected for use in DDS manufacturing in our study. In addition, considering how to administer EPO, we selected intravenous delivery that seemed to be the most convenient approach to systemic circulation administration. For successful DDS administration, the particles must be small enough to pass through lung capillaries. The average diameter of the lung capillary is 3.0 to 13.0  $\mu\text{m}$  in mice and rats and is around 6.3  $\mu\text{m}$  in humans.<sup>39,40</sup> The ferric-ferrous MNPs were found to be 10 nm in diameter.<sup>41</sup> rhEPO is a small, light (30,400 Da) glycoprotein,<sup>8</sup> and the minimum radius of EPO is 2.1 nm, smaller than that of human fibrinogen, based on the Erickson's equation.<sup>42</sup> The intravenous injection of EPO has been shown in numerous rat studies to impart neuro-protective effects.<sup>43,44</sup> In the current experiments, the average diameter of the DDS particles prepared with alginate, EPO, and MNPs was measured to be 0.9  $\mu\text{m}$ , ensuring facile passage through lung capillaries.

## ***3. Limitations of the method***

During the spray drying and encapsulation processing, EPO may become thermally unstable; however, carbohydrate-tagged EPO is expected to display thermal stability up to 56°C, and undergo reversible denaturation below 75°C. This form of EPO regained its conformational stability after cooling.<sup>45</sup> In the current experiments, the temperature of the spray nozzle was 120°C at the inlet and 40°C at the outlet. The DDS solution was sprayed very rapidly (1767

mL/sec) through a very small spray nozzle (4  $\mu\text{m}$ ), and the DDS particles were cooled over 1 hour in a collecting chamber. The EPO subjected to this process was expected to be free from irreversible thermal denaturation. The conformational stability of EPO after processing will be confirmed in future studies, in view of the degree of *in vitro/in vivo* neuro-protective action.

SEM images revealed that the smooth surface of the alginate polymer was converted into a rough surface after spray drying with the MNPs and EPO; however, it was unclear whether the MNPs or EPO formed the rough surface morphology. The ferric-ferrous MNPs were shown to be 10 nm in diameter,<sup>41</sup> and EPO is larger than 4.2 nm in diameter, suggesting that visual differentiation might be difficult using SEM.

High concentrations of EPO beyond a certain threshold can be cytotoxic.<sup>5, 9, 46</sup> Moreover, the degree of neuro-protection by EPO depends on the cell line and nature of the neuronal cell injury.<sup>47</sup> Based on several previous *in vitro* reports with similar study designs,<sup>21, 23, 47</sup> EPO was diluted to an optimal concentration (10 IU/mL) after DDS fabrication. As a result, the concentration of EPO, 0.000084 mg/mL (10 IU), was much lower than that of the MNPs, 1.5 mg/mL, and most of the tiny particles on the rough surfaces of the DDS particles on the SEM were likely to be MNPs, not EPO. At such low concentrations, FTIR spectroscopy was not expected to reveal peaks specific to EPO on the surface. Additionally, the characteristic FTIR spectrum of EPO (chemical formula of EPO:  $\text{C}_{815}\text{H}_{1317}\text{N}_{233}\text{O}_{241}\text{S}_5$ ) has not been reported,<sup>48</sup> and the authors do not at this time have enough information to differentiate the EPO FTIR spectrum from those of alginate and the MNPs.

The cytotoxicity of the ferric-ferrous MNPs obtained after 24 hours incubation at a density of 1500 mg/L using the methods described above (7% lethality) was comparable to the cytotoxicity obtained at much lower concentrations in the report of Mashjoor et al (5% lethality after 24 hours incubation at a density of 100 mg/L).<sup>41</sup> The cytotoxicity was tested here using neuronal cells instead of parasite specie cells. Among the neuronal cells of the CNS, MNP phagocytosis is more likely in PC12<sup>49</sup> and microglia cells.<sup>49</sup> Immune reactions may be precipitated by the presence of MNPs in the CNS.<sup>49</sup> Although neuronal cell toxicity was demonstrated here using SH-SY5Y cells, neuronal toxicity and immune reactions must be assessed in other neuronal cells because no previous reports have tested these properties



in SH-SY5Y cells.

Finally, this study did not analyze the process of EPO release from DDS. Even if the EPO reaches the desired location, it will be ineffective if it does not function in the DDS in a timely manner. It may be necessary to confirm *in vitro* or *in vivo* experiments how to separate from the desired location and how much time is required for release. Previous *in vivo* study using EPO-loaded poly (DL-lactide-co-glycolide) nanoparticles revealed that it was released slowly over 24 hours.<sup>31</sup> But, in the case of spinal cord injury, it should be necessary to release in less time.

#### ***4. Future applications of the method and directions of this research***

Because of its small size, the current DDS could be injected as a solution. After injection, the DDS is anticipated to be concentration within an injured region under a target magnetic field applied using a potentially wearable external magnet. After targeted delivery, spontaneous separation of EPO from the DDS is critical for receptor binding. Alginate maintained its cross-linking stability with the aid of other molecules, such as gelatin or calcium.<sup>50, 51</sup> The spray drying technique has been used previously to fabricate alginate-atenolol microparticles without aiding particles and was, therefore, chosen for use in the current studies.<sup>52</sup> The stability in the human body of the three individual components of the DDS as well as of their composite particles prepared without aiding particles must be evaluated. It may be necessary to introduce additional materials that stabilize the DDS *in vivo* and provide an EPO half-life comparable to that of conventional rhEPO (6-8 hours) with a peak rhEPO presence in the cerebrospinal fluid (CSF) 2 hours after intravenous injection.<sup>43, 53</sup> Whereas DDS particles have been reported to spontaneously break down, the maximum long-term stability of an EPO-polymer (EPO coated with biodegradable gelatin microspheres) was reported to be 8 weeks in an *in vivo* ischemic limb mouse model.<sup>54</sup>

An alternating magnetic field could potentially induce motion among the MNPs inside a DDS. Rapid movement of MNPs under an external high-frequency magnetic field could create heat inside a DDS via piezo-electric effects. This heat could increase the alginate degradation rate. Controlling the alginate degradation rate could potentially control the EPO release rate. In this way, an alternating magnetic field applied to the target area

could control the EPO dose.

Hematopoietic complications, such as teratogenicity, increased viscosity, and thrombosis have been reported.<sup>55</sup> Human studies should seek to avoid these adverse events. Carbamylation has been shown to prevent EPO binding to hematopoietic EPO receptors and preclude hematopoietic activity while still providing neuro-protection in a focal ischemia rat model.<sup>44</sup> Moreover, CNS neuro-protection and –regeneration would require BBB penetration. EPO could be detected in the cisterna magna of rats up to 8 hours after intravenous injection and was found to be present in concentrations comparable to those of simultaneously injected mannitol.<sup>43</sup> Carbamylated non-hematopoietic EPO was also found in the CSF 4–24 hours after intravenous administration in rats.<sup>44</sup>

## CONCLUSIONS

In this study, the authors successfully fabricated a magnetic-guided erythropoietin DDS using the spray-drying technique. In addition, it was confirmed that the erythropoietin DDS was characterized by a size that was small enough to permit passage through lung capillaries while also being susceptible to magnetic guidance. Therefore, the magnetic-guided erythropoietin DDS could be sufficiently applied in *in vivo* and clinical studies. Furthermore, it is expected that its usefulness in the treatment of various CNS injury will be demonstrated.

## REFERENCES

1. Pearse D, Jarnagin K. Abating progressive tissue injury and preserving function after CNS trauma: The role of inflammation modulatory therapies. *Curr Opin Investig Drugs*. 2010;11:1207-1210.
2. Cho YK, Kim G, Park S, Sim JH, Won YJ, Hwang CH et al. Erythropoietin promotes oligodendrogenesis and myelin repair following lysolecithin-induced injury in spinal cord slice culture. *Biochem Biophys Res Commun*. 2012;417:753-759.
3. Juul S. Erythropoietin in the central nervous system, and its use to prevent hypoxic-ischemic brain damage. *Acta Paediatr Suppl*. 2002;91:36-42.
4. Matis GK, Birbilis TA. Erythropoietin in spinal cord injury. *Eur Spine J*. 2009;18:314-323.
5. Morishita E, Masuda S, Nagao M, Yasuda Y, Sasaki R. Erythropoietin receptor is expressed in rat hippocampal and cerebral cortical neurons, and erythropoietin prevents in vitro glutamate-induced neuronal death. *Neuroscience*. 1997;76:105-116.
6. Vitellaro-Zuccarello L, Mazzetti S, Madaschi L, Bosisio P, Gorio A, De Biasi S. Erythropoietin-mediated preservation of the white matter in rat spinal cord injury. *Neuroscience*. 2007;144:865-877.
7. Eid T, Brines M. Recombinant human erythropoietin for neuroprotection: what is the evidence? *Clin Breast Cancer*. 2002;3 Suppl 3:S109-115.
8. Fisher JW. Erythropoietin: physiology and pharmacology update. *Exp Biol Med (Maywood)*. 2003;228:1-14.
9. Hong HN, Shim JH, Won YJ, Yoo JY, Hwang CH. Therapeutic time window for the effects of erythropoietin on astrogliosis and neurite outgrowth in an in vitro model of spinal cord injury. *Medicine (Baltimore)*. 2018;97:e9913.
10. Ehrenreich H, Weissenborn K, Prange H, Schneider D, Weimar C, Wartenberg K et al. Recombinant human erythropoietin in the treatment of acute ischemic stroke. *Stroke*. 2009;40:e647-656.
11. Alibai E, Zand F, Rahimi A, Rezaianzadeh A. Erythropoietin plus methylprednisolone or methylprednisolone in the treatment of acute spinal cord injury: a

preliminary report. *Acta Med Iran.* 2014;52:275-279.

12. Nichol A, French C, Little L, Haddad S, Presneill J, Arabi Y et al. Erythropoietin in traumatic brain injury (EPO-TBI): a double-blind randomised controlled trial. *Lancet.* 2015;386:2499-2506.

13. Dumont F, Bischoff P. Non-erythropoietic tissue-protective peptides derived from erythropoietin: WO2009094172. *Expert Opin Ther Pat.* 2010;20:715-723.

14. Chen H, Spagnoli F, Burris M, Rolland WB, Fajilan A, Dou H et al. Nanoerythropoietin is 10-times more effective than regular erythropoietin in neuroprotection in a neonatal rat model of hypoxia and ischemia. *Stroke.* 2012;43:884-887.

15. Do TD, Ul Amin F, Noh Y, Kim MO, Yoon J. Guidance of Magnetic Nanocontainers for Treating Alzheimer's Disease Using an Electromagnetic, Targeted Drug-Delivery Actuator. *J Biomed Nanotechnol.* 2016;12:569-574.

16. Tietze R, Zaloga J, Unterweger H, Lyer S, Friedrich RP, Janko C et al. Magnetic nanoparticle-based drug delivery for cancer therapy. *Biochem Biophys Res Commun.* 2015;468:463-470.

17. Huq T, Salmieri S, Khan A, Khan RA, Le Tien C, Riedl B et al. Nanocrystalline cellulose (NCC) reinforced alginate based biodegradable nanocomposite film. *Carbohydr Polym.* 2012;90:1757-1763.

18. Majidi S, Sehrig FZ, Farkhani SM, Goloujeh MS, Akbarzadeh A. Current methods for synthesis of magnetic nanoparticles. *Artif Cells Nanomed Biotechnol.* 2016;44:722-734.

19. Mascolo MC, Pei Y, Ring TA. Room Temperature Co-Precipitation Synthesis of Magnetite Nanoparticles in a Large pH Window with Different Bases. *Materials (Basel).* 2013;6:5549-5567.

20. Harsha SN, Aldhubiab BE, Nair AB, Alhaider IA, Attimarad M, Venugopala KN et al. Nanoparticle formulation by Buchi B-90 Nano Spray Dryer for oral mucoadhesion. *Drug Des Devel Ther.* 2015;9:273-282.

21. Li G, Ma R, Huang C, Tang Q, Fu Q, Liu H et al. Protective effect of erythropoietin on beta-amyloid-induced PC12 cell death through antioxidant mechanisms. *Neurosci Lett.* 2008;442:143-147.

22. Ma R, Xiong N, Huang C, Tang Q, Hu B, Xiang J et al. Erythropoietin protects

PC12 cells from beta-amyloid(25-35)-induced apoptosis via PI3K/Akt signaling pathway. *Neuropharmacology*. 2009;56:1027-1034.

23. Zhi-Kun S, Hong-Qi Y, Zhi-Quan W, Jing P, Zhen H, Sheng-Di C. Erythropoietin prevents PC12 cells from beta-amyloid-induced apoptosis via PI3KAkt pathway. *Transl Neurodegener*. 2012;1:7.

24. Xicoy H, Wieringa B, Martens GJ. The SH-SY5Y cell line in Parkinson's disease research: a systematic review. *Mol Neurodegener*. 2017;12:10.

25. Bordbar AK, Rastegari AA, Amiri R, Ranjbakhsh E, Abbasi M, Khosropour AR. Characterization of modified magnetite nanoparticles for albumin immobilization. *Biotechnol Res Int*. 2014;2014:705068.

26. Deepa B, Abraham E, Pothan LA, Cordeiro N, Faria M, Thomas S. Biodegradable Nanocomposite Films Based on Sodium Alginate and Cellulose Nanofibrils. *Materials (Basel)*. 2016;9.

27. Li D, Li P, Zang J, Liu J. Enhanced hemostatic performance of tranexamic acid-loaded chitosan/alginate composite microparticles. *J Biomed Biotechnol*. 2012;2012:981321.

28. Jelkmann W. The enigma of the metabolic fate of circulating erythropoietin (Epo) in view of the pharmacokinetics of the recombinant drugs rhEpo and NESP. *Eur J Haematol*. 2002;69:265-274.

29. Ishii T, Asai T, Urakami T, Oku N. Accumulation of macromolecules in brain parenchyma in acute phase of cerebral infarction/reperfusion. *Brain Res*. 2010;1321:164-168.

30. Wu SK, Yang MT, Kang KH, Liou HC, Lu DH, Fu WM et al. Targeted delivery of erythropoietin by transcranial focused ultrasound for neuroprotection against ischemia/reperfusion-induced neuronal injury: a long-term and short-term study. *PLoS One*. 2014;9:e90107.

31. Fayed BE, Tawfik AF, Yassin AE. Novel erythropoietin-loaded nanoparticles with prolonged in vivo response. *J Microencapsul*. 2012;29:650-656.

32. Wang Y, Cooke MJ, Morshead CM, Shoichet MS. Hydrogel delivery of erythropoietin to the brain for endogenous stem cell stimulation after stroke injury. *Biomaterials*. 2012;33:2681-2692.

33. Zhang W, Gao Y, Zhou Y, Liu J, Zhang L, Long A et al. Localized and sustained

delivery of erythropoietin from PLGA microspheres promotes functional recovery and nerve regeneration in peripheral nerve injury. *Biomed Res Int*. 2015;2015:478103.

34. Zhang W, Zhou G, Gao Y, Zhou Y, Liu J, Zhang L et al. A sequential delivery system employing the synergism of EPO and NGF promotes sciatic nerve repair. *Colloids Surf B Biointerfaces*. 2017;159:327-336.

35. He N, Wang T, Jiang L, Wang D, Hu Y, Zhang L. Therapy for cerebral ischemic injury with erythropoietin-containing nanoparticles. *J Nanosci Nanotechnol*. 2010;10:5320-5323.

36. Khan FA, Almohazey D, Alomari M, Almofty SA. Impact of nanoparticles on neuron biology: current research trends. *Int J Nanomedicine*. 2018;13:2767-2776.

37. Uebe R, Schuler D. Magnetosome biogenesis in magnetotactic bacteria. *Nat Rev Microbiol*. 2016;14:621-637.

38. Shoemaker CB, Mitscock LD. Murine erythropoietin gene: cloning, expression, and human gene homology. *Mol Cell Biol*. 1986;6:849-858.

39. Hafeli UO, Saatchi K, Elischer P, Misri R, Bokharaei M, Labiris NR et al. Lung perfusion imaging with monosized biodegradable microspheres. *Biomacromolecules*. 2010;11:561-567.

40. Townsley MI. Structure and composition of pulmonary arteries, capillaries, and veins. *Compr Physiol*. 2012;2:675-709.

41. Mashjoo S, Yousefzadi M, Zolgharnain H, Kamrani E, Alishahi M. Organic and inorganic nano-Fe<sub>3</sub>O<sub>4</sub>: Alga *Ulva flexuosa*-based synthesis, antimicrobial effects and acute toxicity to briny water rotifer *Brachionus rotundiformis*. *Environ Pollut*. 2018;237:50-64.

42. Erickson HP. Size and shape of protein molecules at the nanometer level determined by sedimentation, gel filtration, and electron microscopy. *Biol Proced Online*. 2009;11:32-51.

43. Ceaglio N, Orozco G, Etcheverrigaray M, Mattio M, Kratje R, Perotti N et al. High performance collection of cerebrospinal fluid in rats: evaluation of erythropoietin penetration after osmotic opening of the blood-brain barrier. *J Neurosci Methods*. 2013;219:70-75.

44. Leist M, Ghezzi P, Grasso G, Bianchi R, Villa P, Fratelli M et al. Derivatives of erythropoietin that are tissue protective but not erythropoietic. *Science*. 2004;305:239-242.

45. Narhi LO, Arakawa T, Aoki KH, Elmore R, Rohde MF, Boone T et al. The effect of carbohydrate on the structure and stability of erythropoietin. *J Biol Chem*. 1991;266:23022-23026.
46. Yoo JY, Won YJ, Lee JH, Kim JU, Sung IY, Hwang SJ et al. Neuroprotective effects of erythropoietin posttreatment against kainate-induced excitotoxicity in mixed spinal cultures. *J Neurosci Res*. 2009;87:150-163.
47. Wu Y, Shang Y, Sun S, Liu R. Antioxidant effect of erythropoietin on 1-methyl-4-phenylpyridinium-induced neurotoxicity in PC12 cells. *Eur J Pharmacol*. 2007;564:47-56.
48. Storring PL, Tiplady RJ, Gaines Das RE, Stenning BE, Lamikanra A, Rafferty B et al. Epoetin alfa and beta differ in their erythropoietin isoform compositions and biological properties. *Br J Haematol*. 1998;100:79-89.
49. Pinkernelle J, Calatayud P, Goya GF, Fansa H, Keilhoff G. Magnetic nanoparticles in primary neural cell cultures are mainly taken up by microglia. *BMC Neurosci*. 2012;13:32.
50. Balakrishnan B, Joshi N, Jayakrishnan A, Banerjee R. Self-crosslinked oxidized alginate/gelatin hydrogel as injectable, adhesive biomimetic scaffolds for cartilage regeneration. *Acta Biomater*. 2014;10:3650-3663.
51. Esser E, Tessmar JK. Preparation of well-defined calcium cross-linked alginate films for the prevention of surgical adhesions. *J Biomed Mater Res B Appl Biomater*. 2013;101:826-839.
52. Ceschan NE, Bucala V, Ramirez-Rigo MV, Smyth HD. Impact of feed counterion addition and cyclone type on aerodynamic behavior of alginic-atenolol microparticles produced by spray drying. *Eur J Pharm Biopharm*. 2016;109:72-80.
53. Jelkmann W. Molecular biology of erythropoietin. *Intern Med*. 2004;43:649-659.
54. Li L, Okada H, Takemura G, Esaki M, Kobayashi H, Kanamori H et al. Sustained release of erythropoietin using biodegradable gelatin hydrogel microspheres persistently improves lower leg ischemia. *J Am Coll Cardiol*. 2009;53:2378-2388.
55. Lippi G, Franchini M, Favaloro EJ. Thrombotic complications of erythropoiesis-stimulating agents. *Semin Thromb Hemost*. 2010;36:537-549.



## APPENDIX

Supplement 1. Characteristic peaks of the nanocomposites in the Fourier-transform infrared spectra.

Peaks ( $\text{cm}^{-1}$ )	Assignments
580 – 630	$\nu(\text{Fe-O})$
1036, 1094	$\nu(\text{C-O})$ ester
1297	$\nu(\text{C-O})$ carboxy
1415, 1613	$\nu(\text{C=O})$
1632	$\delta(\text{O-H})$
2919	$\nu_s(\text{C-H})$
3385	$\nu(\text{O-H})$

## 국문요약

**서문:** Erythropoietin은 2000년대 초부터 중추신경계 손상 실험 모델에서 신경 손상의 억제와 신경 재생을 촉진하는 데 효과가 있음이 알려졌다. 하지만 실제 중추신경계 환자에서 투여하였을 때, 약물작용시간이 짧고, 투여된 약물의 일부만이 수상부위에 작용하는 문제점 등으로 인해 임상적으로는 그 치료효과가 뚜렷하지 못하였다.

하지만 저자들은 최근 대두되고 있는 약물전달시스템(drug delivery system)을 활용한다면 이러한 문제점들을 극복할 수 있을 것으로 판단하였다. 약물전달시스템 기술 중 자성나노입자를 이용한 약물전달시스템은 약물과 자성나노입자를 섞은 다음 약물전달시스템을 신체에 투여하고, 자석을 이용하여 원하는 부위에 이를 전달한 다음 약물을 분리하여 국소적으로 작용케 하는 기술이다. 이번 연구에서 저자들은 자성나노입자를 이용한 Erythropoietin 약물전달시스템의 제작과 임상적인 적용이 실제 가능한지를 실험연구를 통해 먼저 확인하고자 하였다.

**방법** 우선 자성나노입자를 공침법(co-precipitation method)으로 제작하였으며, 이후 나노스프레이 기법을 이용하여 제작된 자성나노입자와 Erythropoietin, 알긴산 나트륨을 섞어 나노마이크로미터 크기의 약물전달시스템을 제작하였다.

제작된 약물전달 시스템은 먼저 주사전자현미경(scanning electron microscopy)을 통해 사람의 혈관을 통과할 수 있는 크기와 모양으로 적절히 제작되었는지를 확인하였다. 그리고 푸리에 변환 적외선 분광법(Fourier-transform infrared spectroscopy)을 이용하여 혼합물이 적절하게 약물전달시스템 내에 섞여 있는지도 확인하였다. 또한 제작된 약물전달시스템이 자석에 의해 잘 이끌리는지를 추가적으로 검증하였다. 검증을 위해 혈관을 모방한 200 $\mu$ m 굵기의 Y형 분기 마이크로채널을 제작하였으며, 채널의 입구로 형광물질을 추가한 약물전달시스템을 투여하고, 두 갈래의 출구 중 한쪽에는 자석을 두어 자석이 있는 방향으로 약물전달시스템이 끌려가는지를 관찰하였다. 마지막으로 Erythropoietin 외에 약물전달시스템을 구성하는 자성나노입자와 알긴산 나트륨이 신경독성이 없는지를 확인하였다. 신경세포인 SH-SY5Y 세포에 자성나노입자, 알긴산 나트륨 그리고 자성나노입자와 알긴산 나트륨을 섞은 혼합물 세가지를 각각 투여한 뒤 이를 24시간 배양하고 세포생존도를 측정하였다.

**결과:** 주사전자현미경상 나노스프레이 기법으로 제작된 약물전달시스템은 500 nm 크기의 구형으로 제작되었음을 확인하였다. 또한 푸리에 변환 적외선 분광법상 약물전달시스템은 자성나노입자와 알긴산 나트륨이 적절히 혼합되어 있음을 확인하였다. 그리고 자석에 대한 이끌림 여부의 검증에서 약물전달시스템이 자석이 위치한 채널의 출구로만 이동함을 확인하였다. 마지막으로 신경독성 여부의 검증에서 자성나노입자, 알긴산 나트륨, 자성나노입자와 알긴산 나트륨 혼합물의 세 가지 조건 모두가 대조군과 비교 시 유의한 생존도의 차이가 관찰되지 않았다.

**결론:** 본 연구에서 저자들은 자성나노입자를 이용한 Erythropoietin 약물전달시스템을 나노스프레이 기법을 이용하여 제작하였다. 또한 제작된 자성나노입자를 이용한 Erythropoietin 약물전달시스템이 추후 *in vivo* 및 임상연구에 충분히 적용할 수 있음을 확인하였으며, 이를 바탕으로 추후 다양한 질환의 치료에서 그 유용성이 증명되기를 기대한다.

**중심단어:** 에리쓰로포이에틴; 자성; 나노입자; 신경독성; 재생